International Journal of Engineering Innovation & Research
Volume 8, Issue 2, ISSN: 2277 – 5668

Measurement and Simulation of the Dent Deformation for Sharp-dented Circular Tubes under Cyclic Bending

Kuo-Long Lee[1] and Wen-Fung Pan[2]
[1]Professor, Dept. of Engineering Science, National Cheng Kung University, Tainan, Taiwan
[2]Professor, Dept. of Innovative Design and Entrepreneurship Management, Far East University, Tainan, Taiwan
Corresponding author email id: z7808034@email.ncku.edu.tw

Date of publication (dd/mm/yyyy): 16/03/2019

***Abstract*– In this paper, the CCD digital camera was used to take photographs of the shape change of the dent for sharp-dented 6061-T6 aluminum alloy tubes subjected to cyclic bending. The dent depths were 0.3, 0.6, 0.9 and 1.2 mm and the controlled curvatures were ±0.35 m^{-1} for cyclic bending. The images taken by the CCD digital camera were analyzed by image processing software from the Matlab to obtain more clear images. In the theoretical simulation aspect, by using proper stress-strain relationship, mesh element, boundary condition and loading condition, the finite element ANSYS was employed to simulate the dent deformation of sharp-dented circular tube subjected to cyclic bending. The analysis cycles included 1^{st}, 5^{th}, 10^{th} and 15^{th} cycles. The deformations at the deepest location of the dent at the negative maximum curvature (-0.35 m^{-1}) subtracted the deepest location of the dent at positive maximum curvature (+0.35 m^{-1}) to obtain the amount of the maximum deformation at the dent. Finally, the images taken by the CCD digital camera were compared with the ANSYS simulation. It is shown that the theoretical simulation can properly represent the experimental results.**

***Keywords* –Sharp-dented 6061-T6 Aluminum Alloy Tubes, Cyclic Bending, CCD Digital Camera, Finite Element ANSYS Analysis.**

I. INTRODUCTION

In 2000, Corona and Kyriakides [1] investigated the pipe buckling under pure bending with some external pressure. Corona, Lee and Kyriakides [2] found that the tubes exhibited the plastic anisotropy, and the group measured and characterized this anisotropy using Hill's yield function. Thereafter, Limam, Lee, Corana and Kyriakides [3] studied the inelastic bending and collapse of tubes under internal pressure using experiments and analyses. Limam, Lee and Kyriakides [4] also experimentally and analytically studied the effect of local dents on the collapse curvature of pressurized pipes submitted to bending. Bechle and Kyriakides [5] later investigated the localization of NiTi tubes under bending, as well as the influence of the texture-driven and complex material asymmetry on a simple structure. Jiang, Kyriakides, Bechleand Landis [6] used a constitutive model in a finite element analysis for describing the pseudoelastic behavior of NiTi tubes subjected to bending.

Several other scholars have published related studies. Elchalakani, Zhao and Grzebieta [7] experimentally conducted tests on different diameter-to-thickness ratios of grade C350 steel tubes subjected to bending. Jiao and Zhao [8] tested the bending behavior of very-high-strength circular steel tubes. Elchalakani, Zhao and Grzebieta [9] conducted variable amplitude, cyclic bending tests to determine fully ductile section slenderness limits for the cold-formed CHS. Elchalakani and Zhao [10] investigated concrete-filled cold-formed circular steel tubes under variable-amplitude cyclic pure bending. Yazdani and Nayebi [11] investigated the ratcheting and fatigue damage of thin-walled tubes subjected to cyclic bending with a steady internal pressure. Elchalakani, Karrech¸ Hassanein and Yang [12] employed the measured strain in plastic bending tests to determine new ductile slenderness limits

for the plastic design of CFT structures. Shamass, Alfano and Guarracino [13] studied the elastoplastic buckling of thin circular shells subjected to a non-proportional loading.

In 1998, Pan, Wang and Hsu [14] designed and set up a new measurement apparatus. The apparatus was used with a cyclic bending machine to study various types of tube under different cyclic bending conditions. For examples: Pan and Her [15] investigated the response and stability of 304 stainless steel tubes that were subjected to cyclic bending with different curvature rates, Chang and Pan [16] discussed the buckling life estimation of circular tubes subjected to cyclic bending.

In 2010, the research team of Prof. Pan began to experimentally and analytically investigate the response and the collapse of sharp-notched circular tubes submitted to cyclic bending. Lee, Hung and Pan [17] experimentally studied the relationship between the variation of ovalization and the number of bending cycles for sharp-notched circular tubes subjected to cyclic bending. They discovered that the aforementioned relationship could be clearly divided into three stages, namely initial, secondary, and tertiary. Lee, Hsu and Pan [18] evaluated the viscoplastic response and buckling of sharp-notched SUS304 stainless steel circular tubes undertaking cyclic bending. Both the different notch depths and curvature rate were examined. Chung, Lee and Pan [19] investigated the response and stability of sharp-notched 6061-T6 aluminum alloy tubes under cyclic bending. However, the sharp notch for the aforementioned studies was a circumferential sharp notch as shown in Fig. 1.

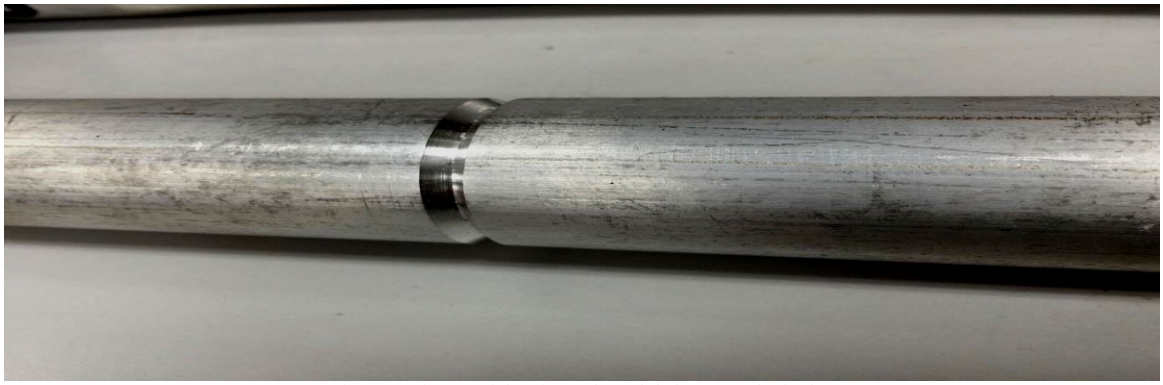

Fig. 1. A picture of the circumferential sharp-notched tube.

In this paper, the tube-bending machine was used to conduct cyclic bending tests on sharp-dented 6061-T6 aluminum alloy tubes with different dent depths. The CCD digital camera measurement system [20] was used to take photographs of the shape changes of sharp dents during the test. Next, by using Matlab image processing software, clearer dent shape images were obtained. According to the actually captured image position, the maximum change in dent deformation was determined. Finally, the finite element ANSYS analysis was employed to simulate the shape changes of sharp dents for sharp-dented 6061-T6 aluminum alloy tubes with different dent depths under cyclic bending. Simultaneously, the maximum deformations of the sharp dents were obtained. In addition, the experimental measurement was compared with the ANSYS simulation.

II. EXPERIMENT

A. *Tube-bending Machine*

Fig. 2 schematically shows the experiments executed by a specially built tube-bending machine. This facility was built to conduct monotonic, reverse, and cyclic bending tests. A detailed explanation of the experimental facility can be found in many papers (Pan, Wang and Hsu [14], Pan and Her [15]).

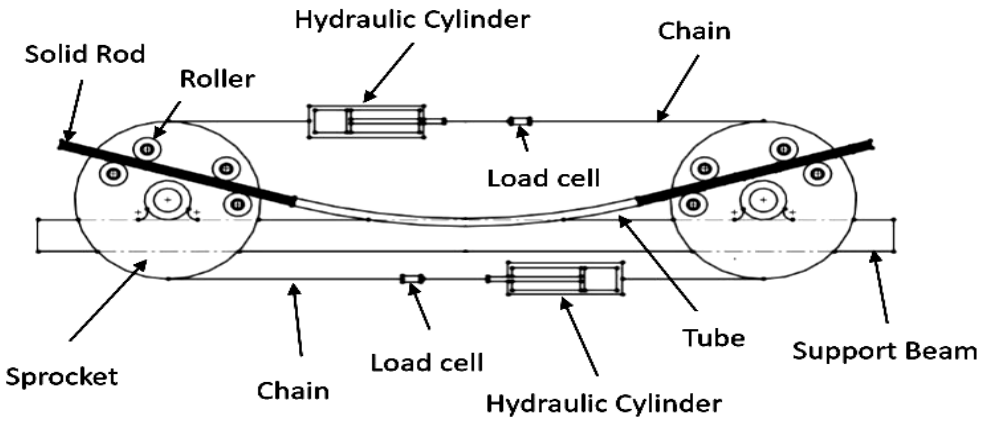

Fig. 2. A schematic drawing of the tube-bending machine.

B. *CCD Digital Camera Measurement System*

Fig. 3 shows the CCD digital camera measurement system designed by Lee, Hung and Pan [20], which includes a CCD digital camera, a supporting bracket and two inclinometers. The supporting bracket contains the following three parts. (1) A stretchable CCD camera supporting bracket - The position of the bracket can be adjusted according to the characteristic of the CCD digital camera. (2) A stretchable light supporting bracket - A suitable light can be set up on the bracket. According to the required intensity of light, the positioning of the light can be adjusted. (3) A strong clamp - Because the circular tube may move up and down during cyclic bending, a slice movement of the bracket may cause distortion of the detected image.

When a tube is subjected to cyclic bending, the CCD digital camera starts to take photographs of tube deformation. The images from the CCD digital camera are imported to Matlab image processing software. Clearer deformation of the tube can be determined. In addition, there are two inclinometers fixed on the tube by two clamps. The tube curvature can be determined by a simple calculation according to the angle changes. An extended version of the calculation can be found in the work by Lee, Hung and Pan [20].

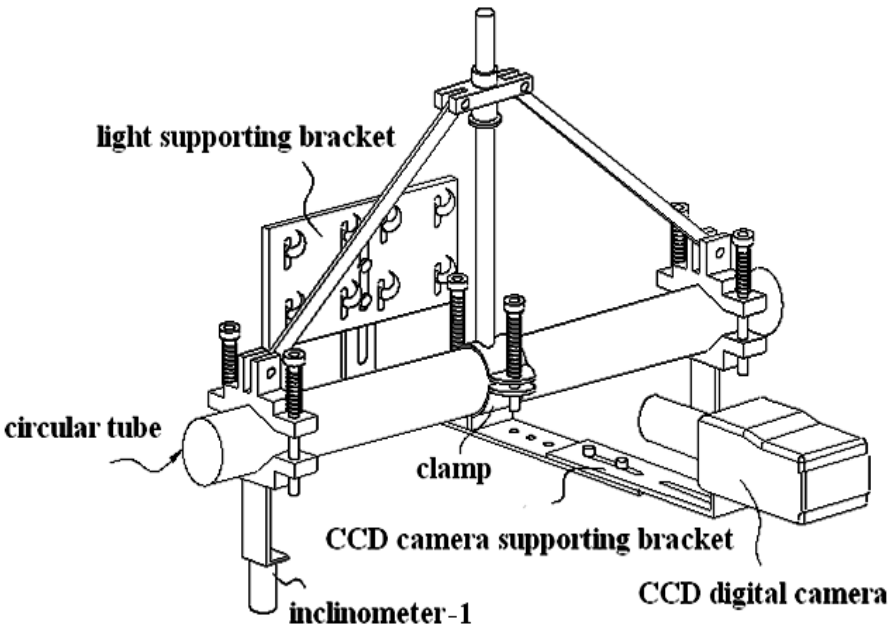

Fig. 3. CCD digital camera measurement system.

C. *Material and Specimens*

Circular tubes made of 6061-T6 aluminum alloy were adopted in this study. Table 1 shows the alloy's chemical composition in weight percentage. The ultimate stress is 258 MPa, the 0.2% strain offsetting yield stress is 166 MPa, and the percent elongation is 23%.

Table 1 - Chemical composition of 6061-T6 aluminum alloy (weight %).

Chemical Composition	Al	Mg	Si	Ti	Fe
Proportion (%)	98.096	0.937	0.535	0.012	0.139
Chemical Composition	Mn	Zn	Cr	Ni	
Proportion (%)	0.022	0.0983	0.022	0.005	

The original tubes with an outside diameter D_o of 33.0 mm and a wall thickness t of 2.0 mm were processed on the outside surface to create the expected dents. Figs. 4(a) and 4(b) show a picture and a schematic drawing of the dent production, respectively. The indenter contacted the outside surface and exerted a force F to create a dent. Four different dent depths (a) were considered herein: 0.3, 0.6, 0.9, and 1.2 mm.

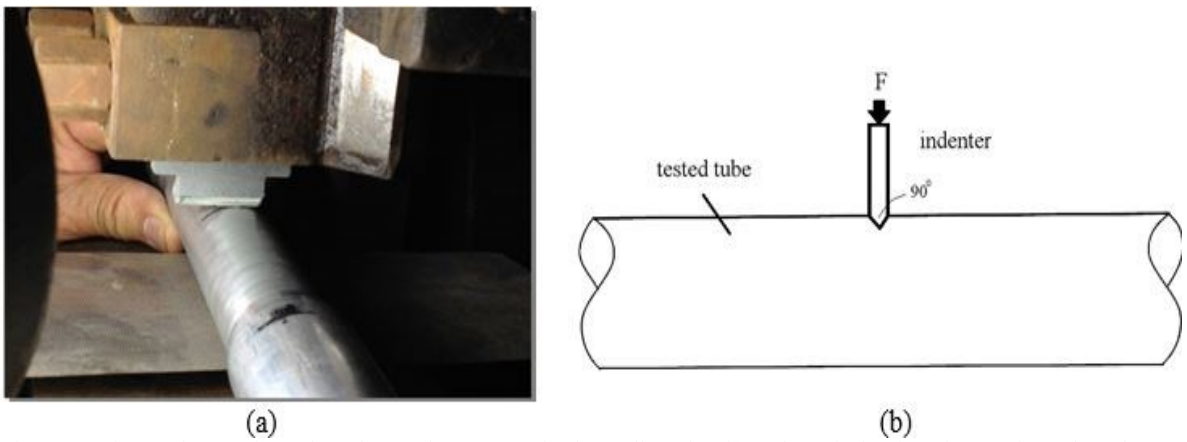

Fig.4. (a)A picture of processing a sharp dent on the 6061-T6 aluminum alloy tube, (b) a schematic drawing of processing a sharp dent on the 6061-T6aluminum alloy tube.

D. *Test Procedures*

The test involved a curvature-controlled cyclic bending. The curvature rate of the cyclic bending test was 0.0035 $m^{-1}s^{-1}$. The magnitude of the curvature and dent deformation of the tube were controlled and measured by the CCD digital camera measurement system. In addition, the number of cycles was recorded.

III. FINITE ELEMENT ANSYS ANALYSIS

In this study, the response of locally-dented circular tubes subjected to cyclic bending was also analyzed numerically using the finite element code ANSYS. The response is the correlation between the deformation and curvature. The elastic-plastic stress-strain response, model, mesh, boundary condition, and loading condition are explained below.

A. *Elastic-plastic Stress-strain Curves*

Fig. 5 shows the tested and ANSYS-constructed uniaxial stress (σ) - strain (ε) curves for the 6061-T6 aluminum alloy. The kinematic hardening rule was used as the hardening rule for cyclic loading.

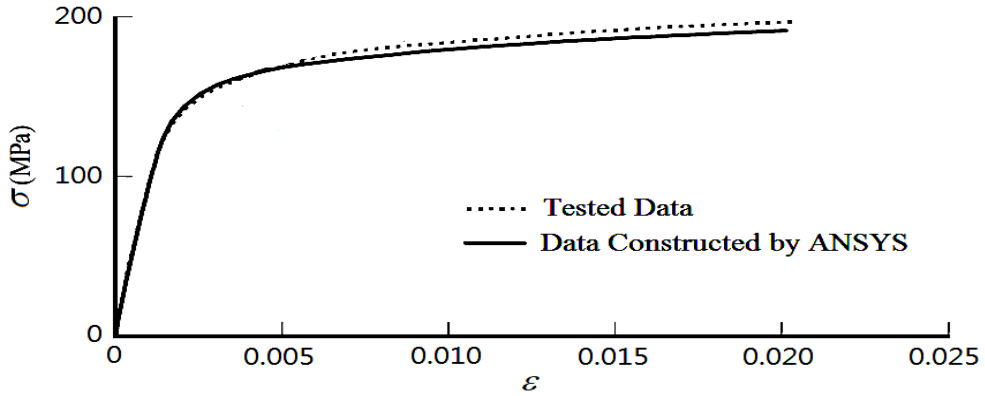

Fig.5. Tested and ANSYS constructed data of the uniaxial stress (σ) - strain (ε) curves for 6061-T6 aluminum alloy.

B. *Model*

The model consisted of three parts: the locally-dented tube, the indenter, and the solid rod. The size and geometric shape of the locally-dented tube are stated in a previous section and the schematic drawings of the indenter and solid rod are shown in Figs. 6(a) and 6(b), respectively. It can be seen in Fig. 6(a) that production of a dent includes the indenter and a fixed plate. The indenter exerts a pressure on the tube related to the desired depth of the dent. The shape and size of the dents are discussed in a previous section.

C. *Mesh*

Due to the three-dimensional geometry and elastic-plastic deformation of the tube, the SOLID 185 element was used for relative analysis. This is a tetrahedral element built in ANSYS and is suitable for analyzing plastic or large deformations. In particular, the element can adequately analyze shell components under bending. Due to the right and left symmetry, only half of the tube model was constructed. Fig. 7(a) shows the mesh constructed by ANSYS for the indenter and half tube, and Fig. 7(b) shows the mesh constructed by ANSYS for the half tube.

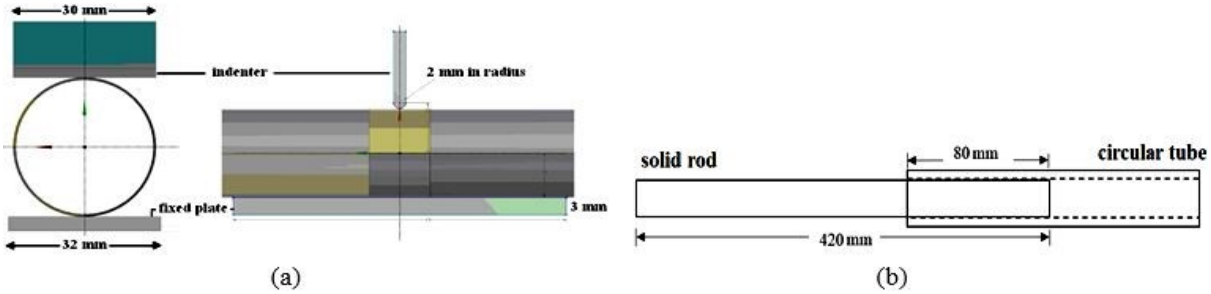

Fig.6. Schematic drawings of (a) the indenter and (b) solid rod.

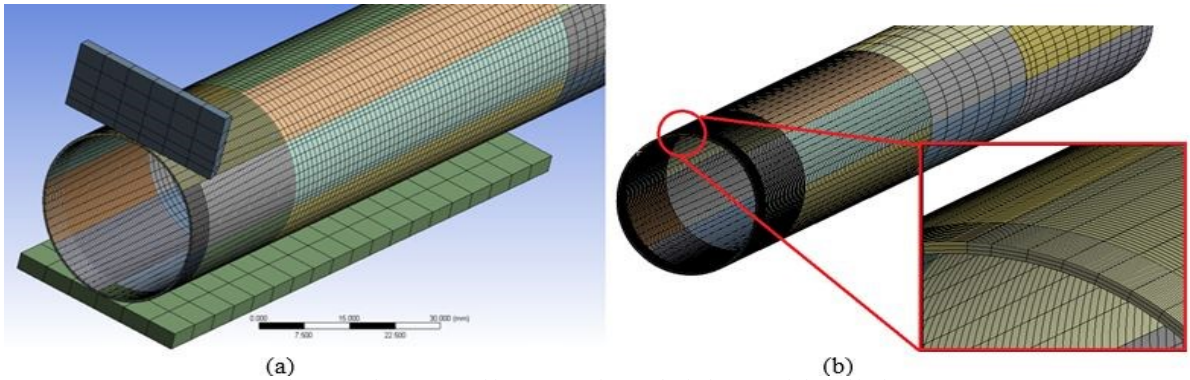

Fig. 7. Mesh constructed by ANSYS for (a) the indenter and (b) half tube.

D. *Boundary Condition*

When producing a dent on the tube, the indenter moved in the y-direction only. Therefore, friction supports were set to prevent any displacement in the x- or z-directions, as shown in Fig. 8(a). The indenter was set to exert pressure on the tube to produce a dent and then to reset back to its original position. The contact between the indenter and tube was set to be frictionless shown in Fig. 8(b). The plate was fixed, thus, a fixed support was set on the plate shown in Fig. 9(a). As there was no related displacement between the tube and the fixed plate, the bonded contact between them was used shown in Fig. 9(b).

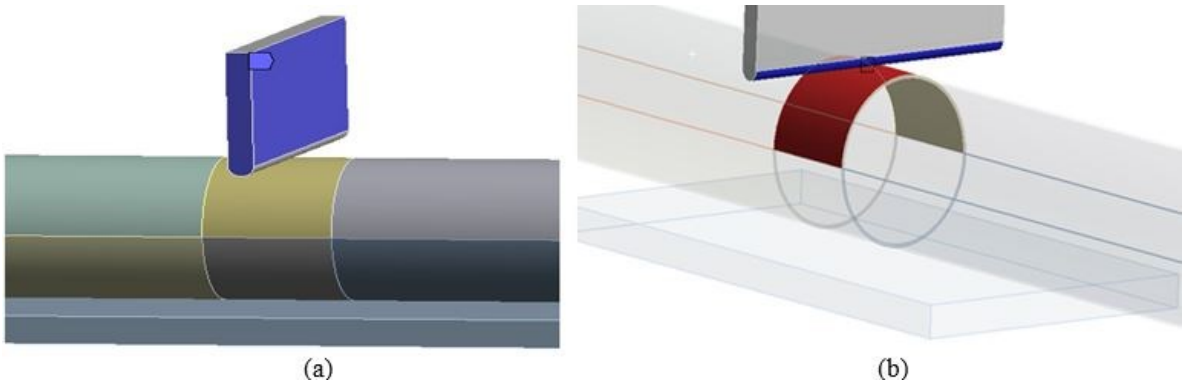

Fig. 8. Boundary condition for (a) the indenter and (b) contact between the indenter and tube.

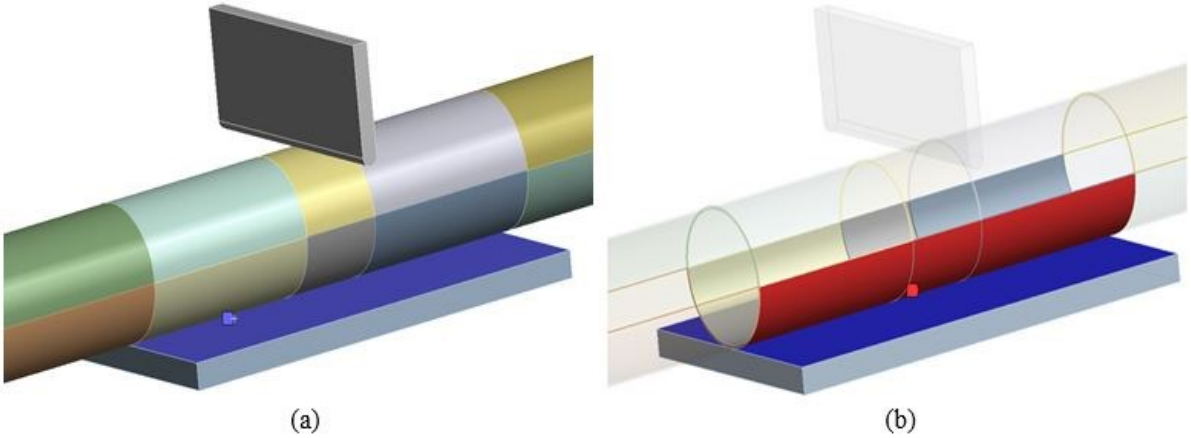

Fig. 9. Boundary condition for (a) the fixed plate and (b) contact between the tube and fixed plate.

E. *Loading Condition*

When producing a dent, the indenter was set to move downward to create a desired dent depth, then travel back to its original position. Fig. 10(a) shows the loading conditions of the indenter as constructed by ANSYS. Fig. 10(b) shows the loading condition constructed by ANSYS on the basis of the tube-bending device. As shown, the remote displacement of the solid rod in the z-direction was unrestricted, i.e., the rotation was free to move in the z-direction. In addition, the bending moment was applied only in the z-direction, hence, the rotations in the x- and y-directions were set to zero.

Fig. 11 depicts a tube subjected to pure bending. The rotating angle θ was used as input data for curvature-controlled cyclic bending. The curvature κ is

$$\kappa = 1/\rho = 2\theta/L_o, \qquad (1)$$

where ρ is the radius of curvature and L_o is the original tube length.

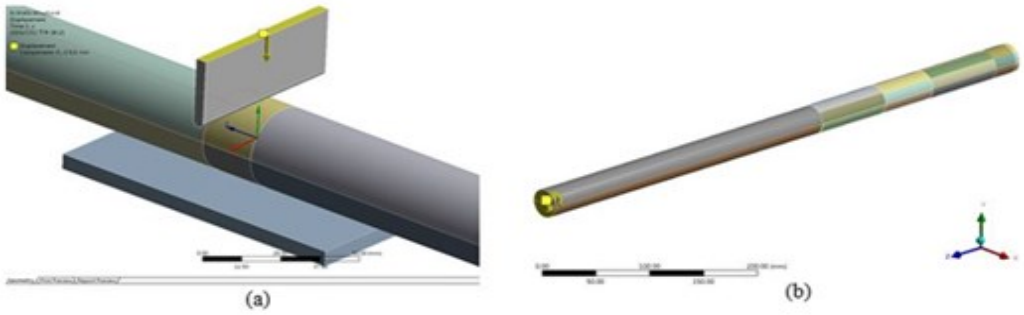

Fig. 10. Loading condition for (a) the indenter and (b) solid rod.

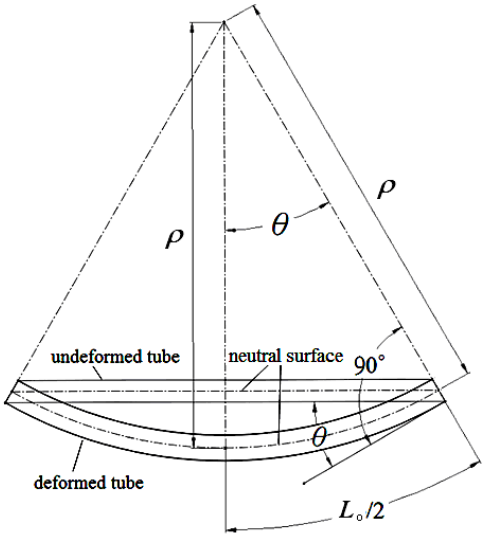

Fig. 11. Relationship between θ and κ for a tube under pure bending.

IV. Results and Discussion

A. *Shooting and Image Processing*

Figs. 12(a)-(e) respectively show dent images of sharp-dented 6061-T6 aluminum alloy tubes with a = 1.2 mm under cyclic bending at 0, 1/4, 2/4, 3/4 and 1st cycle. Then, the dent images captured by the CCD digital camera measurement system were obtained by using the canny edge detection method built in Matlab software and the Photoshop software sharpening mask, etc. By properly processing each image, lines with only edges were observed, as shown in Figs. 13(a)-(e).

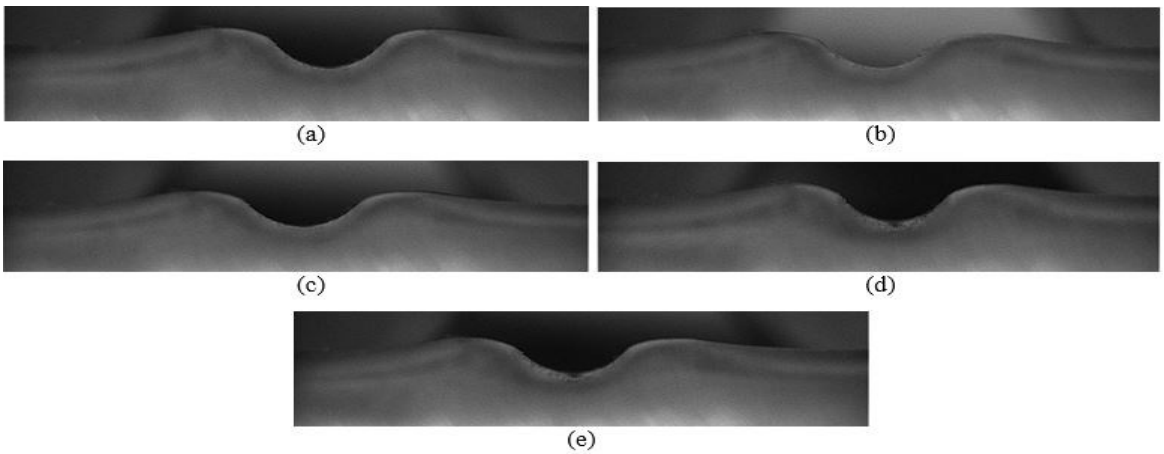

Fig.12. Dent images captured by the CCD digital camera measurement system of sharp-dented 6061-T6 aluminum alloy tubes with a = 1.2 mm under cyclic bending at (a) 0, (b) 1/4, (c) 2/4, (d) 3/4 and (e) 1st cycle.

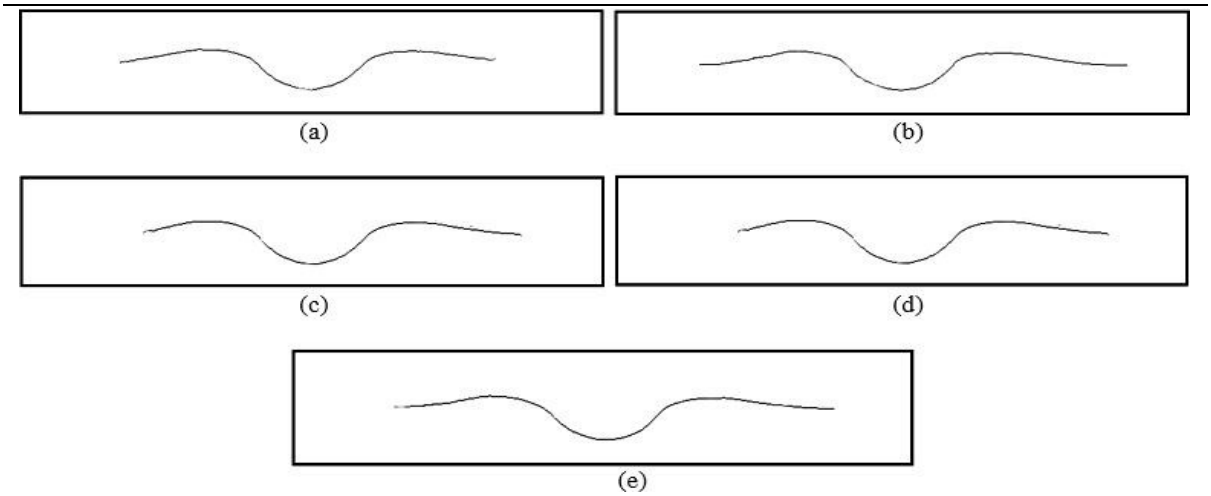

Fig.13. Dent images by the image processing of sharp-dented 6061-T6 aluminum alloy tubes with a = 1.2 mm under cyclic bendingat (a) 0, (b) 1/4, (c) 2/4, (d) 3/4 and (e) 1st cycle.

B. *Comparison of CCD Digital Camera Measurement and ANSYS Analysis*

Fig. 14(a) shows overlapping of the dent edges after image processing at the 0, 1/4, 2/4, 3/4 and 1st cycle of the sharp-dented 6061-T6 aluminum alloy tube with a = 1.2 mm under cyclic bending. The scale of the ordinate was enlarged by 8 times, and yellow, purple, green, red and blue lines represented the dent edges at 0, 1/4, 2/4, 3/4 and 1st cycle, respectively. The figure shows that when the tube is bent to a curvature of +0.35 m^{-1}, the depth of the dent is reduced from 1.2 mm to 1.167 mm (1/4 cycle), and when the tube is bent to a curvature of -0.35 m^{-1}, the depth of the dent increases from 1.167 mm to 1.278 mm (3/4 cycle). Fig. 14(b) shows overlapping of the dent edges after ANSYS analysis at the 0, 1/4, 2/4, 3/4 and 1st cycle of the sharp-dented 6061-T6 aluminum alloy tube with a = 1.2 mm under cyclic bending. The scale of the ordinate was also enlarged by 8 times, and yellow, purple, green, red and blue lines represented dent edges at 0, 1/4, 2/4, 3/4 and 1st cycle, respectively. The figure shows that when the tube is bent to a curvature of +0.35 m^{-1}, the depth of the dent is reduced from 1.2 mm to 1.160 mm (1/4 cycle), and when the tube is bent to a curvature of -0.35 m^{-1}, the depth of the dent increases from 1.160 mm to 1.265 mm (3/4 cycle).The enlarged illustration in the lower right corner shows the loading process for the first cycle, which is the 0 →1/4 →2/4 →3/4 →1st cycle.

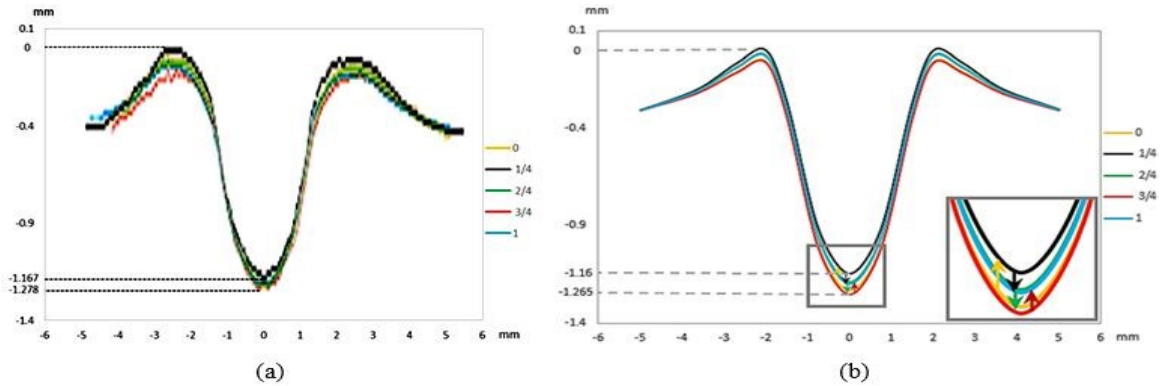

Fig.14. Overlapping of the dent edge after (a) image processing and (b) ANSYS analysis at the 0, 1/4, 2/4, 3/4 and 1st cycle of the sharp-dented 6061-T6 aluminum alloy tube with a = 1.2 mm under cyclic bending.

C. *Relationship between the Maximum Deformation of the Dent and the Number of Cycles*

The maximum deformation of the dent (δ_T) was defined as the amount of dent deformation at the maximum negative control curvature (-0.35 m^{-1}) minus that at the maximum positive control curvature (+0.35 m^{-1}). The

shooting cycles in this experiment were at 1th, 5th, 10th and 15th cycles. Figs. 15(a)-(d) respectively demonstrate δ_T-N relationships of sharp-dented 6061-T6 aluminum alloy tubes with a = 0.3, 0.6, 0.9 and 1.2 mm under cyclic bending. The figures show that when the a is shallow, the δ_T is relatively small, and the δ_T is relatively large when a is deep. For example, when N = 1, the δ_T corresponding to a = 0.3, 0.6, 0.9, and 1.2 mm are 0.025, 0.0445, 0.079, and 0.111 mm, respectively. In addition, the distribution of δ_T is roughly larger at the 1st cycle, and then gradually becomes smaller as N increases. As for the δ_T (Fig. 15(a)) with a = 0.3 mm, it gradually becomes larger as N increases, possibly because the amount of dent change is too small, resulting in an error in the measurement. As for the δ_T (Fig. 15(d)) with a = 1.2 mm, the difference between the experiment and the ANSYS analysis is very large at the 15th cycle. The main reason is that the fatigue life of the tube is 16 cycles, cracks have appeared on the dent at the 15th cycle, and the model of ANSYS analysis does not consider the situation when the crack occurs, so there will be a big difference between the two.

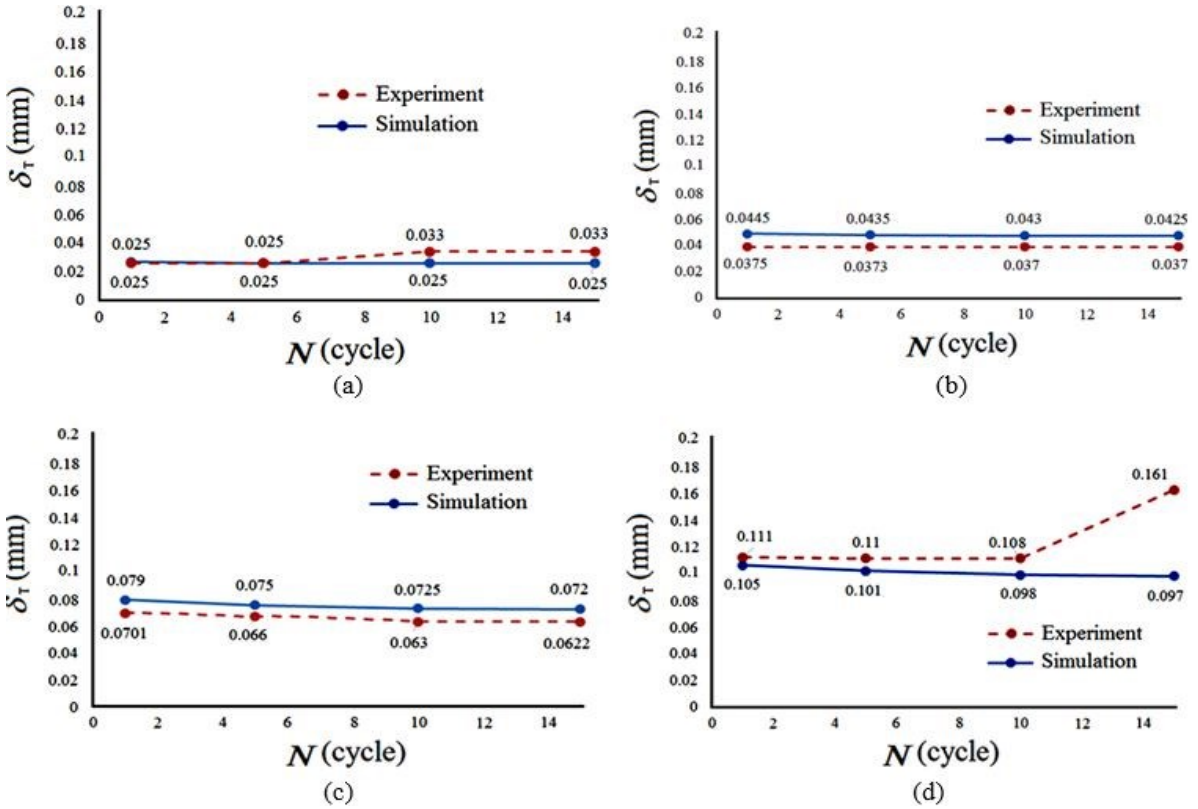

Fig.15. The maximum deformation of dents (δ_T) and number of cycles (N) of sharp-dented 6061-T6 aluminum alloy tubes with a = (a) 0.3, (b) 0.6, (c) 0.9 and (d) 1.2 mm under cyclic bending.

V. CONCLUSION

This study is an experimental measurement and theoretical simulation of variation of dent deformations for sharp-dented 6061-T6 aluminum alloy tubes with different as under cyclic bending. The CCD digital camera measurement system was used to experimentally shoot the sharp dents and the captured images were transmitted through the image processing software in Matlab to obtain clearer images of the dent shapes. The finite element analysis ANSYS was used to perform the relevant theoretical simulations. The ANSYS analysis of the δ_T-N relationships for sharp-dented 6061-T6 aluminum alloy tubes with a = 0.3, 0.6, 0.9 and 1.2 mm under cyclic bending were compared with the experimental measurement (Figs. 15(a)-(d)). Good agreement between the experimental measurement and ANSYS-simulated results has been achieve.

ACKNOWLEDGEMENT

The work presented was carried out with the support of the National Science Council under grant MOST 105-2221-E-006-073. Its support is gratefully acknowledged.

REFERENCES

[1] E. Corona, and S. Kyriakides, "Asymmetric collapse modes of pipes under combined bending and pressure," *Int. J. Solids Struct.*, vol. 24, no. 5, 2000, pp. 505-535.
[2] E. Corona, L.-H. Lee, and S. Kyriakides, "Yield anisotropic effects on buckling of circular tubes under bending," *Int. J. Solids Struct.*, vol. 43, no. 22, 2006, pp. 7099-7118.
[3] A. Limam, L.-H. Lee, E. Corana, and S. Kyriakides, "Inelastic wrinkling and collapse of tubes under combined bending and internal pressure," *Int. J. Mech. Sci.*, vol. 52, no. 5, 2010, pp. 37-47.
[4] A. Limam, L.-H. Lee, and S. Kyriakides, "On the collapse of dented tubes under combined bending and internal pressure," *Int. J. Solids Struct.*, vol. 55, no. 1, 2012, pp. 1-12.
[5] N. J. Bechle, and S. Kyriakides, "Localization of NiTi tubes under bending," *Int. J. Solids Struct.*, vol. 51, no. 5, 2014, pp. 967-980.
[6] D. Jiang, S. Kyriakides, N. J. Bechleand C. M. Landis, "Bending of pseudoelastic NiTi tubes," *Int. J. Solids Struct.*, vol. 124, 2017, pp. 192-214.
[7] M. Elchalakani, X.-L. Zhao and R.H. Grzebieta, "Plastic mechanism analysis of circular tubes under pure bending," *Int. J. Mech. Sci.*, vol. 44, no. 6, 2002, pp. 1117-1143.
[8] H. Jiao and X.-L. Zhao, "Section slenderness limits of very high strength circular steel tubes in bending," *Thin-Walled Struct.*, vol. 42, no. 9, 2004, pp. 1257-1271.
[9] M. Elchalakani, X.-L. Zhao and R. H. Grzebieta, "Variable amplitude cyclic pure bending tests to determine fully ductile section slenderness limits for cold-formed CHS," *Eng. Struct.*, vol. 28, no. 9, 2006, pp. 1223-1235.
[10] M. Elchalakani and X.-L. Zhao, "Concrete-filled cold-formed circular steel tubes subjected to variable amplitude cyclic pure bending," *Eng. Struct.*, vol. 30, no. 2, 2008, pp. 287-299.
[11] H. Yazdani and A. Nayebi, "Continuum damage mechanics analysis of thin-walled tube under cyclic bending and internal constant pressure,"*Int. J. Appl. Mech.*, vol. 5, no. 4, 2013, 1350038 [20 pages].
[12] M. Elchalakani, A. Karrech and M. F. Hassanein and B. Yang, "Plastic and yield slenderness limits for circular concrete filled tubes subjected to static pure bending," *Thin-Walled Struct.*, vol. 109, 2016, pp. 50-64.
[13] R. Shamass, G. Alfano and F. Guarracino, "On elastoplastic buckling analysis of cylinders under nonproportional loading by differential quadrature method," *Int. J. Struct. Stab. Dyn.*, vol. 17, no. 7, 2017, 1750072 [40 pages].
[14] W.-F. Pan, T.-R. Wang, and C.-M. Hsu, "A curvature-ovalization measurement apparatus for circular tubes under cyclic bending,"*Exp. Mech.*, vol. 38, no. 2, 1998,pp. 99-102.
[15] W.-F. Pan, and Y.-S. Her, "Viscoplastic collapse of thin-walled tubes under cyclic bending," *ASME J. Eng. Mat. Tech.*, vol. 120, no. 4, 1998, pp. 287-290.
[16] K.-H. Chang, and W.-F. Pan, "Buckling life estimation of circular Tubes under Cyclic Bending,"*Int. J. Solids Struct.*, vol. 46, no. 2, 2009, pp. 254-270.
[17] K.-L. Lee, C.-Y. Hung, and W.-F. Pan, "Variation of ovalization for sharp-notched circular tubes under cyclic bending,"*J. Mech.*, vol. 26, no. 3, 2010, pp. 403-411.
[18] K.-L. Lee, C.-M. Hsu, and W.-F. Pan, "Viscoplastic collapse of sharp-notched circular tubes under cyclic bending,"*Acta Mech. Solida Sinica*, vol. 26, no. 6, 2013,pp. 629- 641.
[19] C.-C. Chung, K.-L. Lee, and W.-F. Pan, "Collapse of sharp-notched 6061-T6 aluminum alloy tubes under cyclic bending," *Int. J. Struct. Stab. Dyn.*, vol. 16, no. 7, 2016,1550035 (24 pages).
[20] K.-L. Lee, C.-Y. Hung and W.-F. Pan, "CCD digital camera system for measuring curvature and ovalization of each cross-section of circular tubes under cyclic bending," *J. Chi. Inst. Eng.*, vol. 34, no. 1, 2011, pp. 75-86.

AUTHORS PROFILE'

Kuo-Long Lee received the Ph.D. degree in Dept. of Engineering Science from National Cheng Kung University in Taiwan in 2000. Currently working as Prof. in Dept. of Innovative Design and Entrepreneurship from Far East University in Taiwan

Wen-Fung Pan received the Ph.D. degree in Dept. of Civil and Environmental Engineering from University of Iowa in USA in 1989. Currently working as Prof. in Dept. of Engineering Science from National Cheng Kung University in Taiwan.